Ground Penetrating Radar Survey in Search of Fort Mathews, 9OC43, Oconee County, Georgia

LAMAR Institute Publication Series, Report Number 192

Savannah, Georgia

2014

Ground Penetrating Radar Survey in Search of Fort Mathews, Oconee County, Georgia

LAMAR Institute Publication Series,

Report Number 192

By Daniel T. Elliott

The LAMAR Institute, Inc.

Savannah, Georgia

2014

Introduction

This report details the Ground Penetrating Radar Survey of a sample portion of Archaeological Site 9OC43. Site 9OC43 is recorded in the Georgia Archaeological Site File (GASF) as the suspected site of Fort Mathews (Ledbetter 1981). The site is located on a small knoll above the Oconee River floodplain on the east side of the Oconee River in rural Oconee County, Georgia. Whether this site is indeed the 1790s fort site remains a subject of some debate. Recent archaeological exploration by O'Steen (2012) has demonstrated that the site contains artifacts from the same time range as the fort (ca. 1780-1810), although objects of a distinct military character have not been identified. O'Steen assembled historical documents and oral traditions in her search for Fort Mathews and a broader study of the Barnett Shoals vicinity. The 1980 oral account of John Aubryne Kennedy, since deceased, identified the 9OC43 location as Fort Mathews. Georgia's Adjutant General Augustus Elholm personally reviewed the fortifications on the middle and upper Oconee River region in 1793 and he left us with an overview sketch map showing the relative locations of most of these forts. Other maps by Jonas Fauche and another unidentified draftsperson show fortifications in the Oconee River region in similar crude detail. No contemporary detailed drawings or verbal descriptions of Fort Mathews have been located.

Fort Mathews was a frontier fort that was garrisoned by Georgia militia and U.S. Army troops between 1791 and1794 (O'Steen 2012). The fort housed approximately two dozen troops in the few years it was occupied. Ground Penetrating Radar (GPR) was seen as a technology that could be employed in an attempt to solve the Fort Mathews mystery. One day was devoted to a sample GPR survey of a portion of 9OC43 and the results of this research effort are detailed in this report.

Figure 1. Location Map, 9OC43.

Methods

The equipment used for the GPR survey at 9OC43 consisted of a RAMAC/X3M Integrated Radar Control Unit, mounted on a wheeled-cart and linked to a RAMAC XV11 Monitor (Firmware, Version 3.2.36). A 500 megahertz (MHz) shielded antenna was used for the data gathering. MALÅ GeoScience's Ground Vision software (Version 1.4.6) was used to acquire and record the radar data (MALÅ GeoScience USA 2006). The radar information was displayed as a series of radargrams. Output from the survey was first viewed using GroundVision. This provided immediate feedback about the suitability of GPR survey in the area and the effective operation of the equipment. GPR-Slice software (Version 7.0) was used in post-processing the data.

The same RAMAC X3M GPR system as that used in the present study has been used successfully by the author on numerous archaeological sites in the southeastern United States. The methods employed for the GPR survey were consistent with similar projects conducted by the LAMAR Institute.

Ground Penetrating Radar (GPR) is an important remote-sensing tool used by archaeologists (Conyers and Goodman 1997). The technology is particularly effective in mapping historic cemeteries. The technology uses high frequency electromagnetic waves (microwaves) to acquire subsurface data. The device uses a transmitter antenna and closely spaced receiver antenna to detect changes in electromagnetic properties beneath them. The antennas are suspended just above the ground surface and are shielded to eliminate interference from sources other than directly beneath the device. The transmitting antenna emits a series of electromagnetic microwaves, which are distorted by differences in soil conductivity, dielectric permitivity, and magnetic permeability. The receiving antenna records the reflected waves for a specified length of time (in nanoseconds, or ns). The approximate depth of an object can be estimated with GPR, by adjusting for electromagnetic propagation conditions.

The GPR samples in this study area were composed of a series of parallel transects, or traverses, which yielded a two-dimensional cross-section or profile of the radar data. These samples are termed radargrams. This two-dimensional image is constructed from a sequence of thousands of individual radar traces. A succession of radar traces bouncing off a large buried object will produce a hyperbola, when viewed graphically in profile. Multiple large objects that are in close proximity may produce multiple, overlapping hyperbolas, which are more difficult to interpret.

The GPR signals that are captured by the receiving antenna are recorded as an array of numerals, which can be converted to gray scale (or color) pixel values. The radargrams are essentially a vertical map of the radar reflection off objects and other soil anomalies. It is not an actual map of the objects. The radargram is produced in real time and is viewable on a computer monitor, mounted on the GPR cart.

GPR has been successfully used for archaeological and forensic anthropological applications to locate relatively shallow features, although the

technique also can probe deeply into the ground. The machine is adjusted to probe to the depth of interest by the use of different frequency range antennas. Higher frequency antennas are more useful at shallow depths, which is most often the case in archaeology. Also, the longer the receiving antenna is set to receive GPR signals (measured in nanoseconds, or ns), the deeper the search. The effectiveness of GPR in various environments on the North American continent is widely variable and depends on solid conductivity, metallic content, and other pedo-chemical factors.

GPR signals cannot penetrate large metal objects and the signals are also significantly affected by the presence of salt water. Although radar does not penetrate metal objects, it does generate a distinctive signal that is usually recognizable, particularly for larger metal objects, such as a cast iron cannon or man-hole cover. The signal beneath these objects is often canceled out, which results in a pattern of horizontal lines on the radargram. For smaller objects, such as a scatter of nails, the signal may ricochet from the objects and produce a confusing signal. Rebar-reinforced concrete, as another example, generates an unmistakable radar pattern of rippled lines on the radargram.

The time window that was selected allowed data gathering to focus on the upper 1.5 meters of soil, which was the zone most likely to yield archaeological deposits. Additional filters were used to refine the radar information during post-processing. These include adjustments to the gain. These alterations to the data are reversible, however, and do not affect the original data that was collected.

Upon arrival at the site the RAMAC X3M Radar Unit was set up for the operation and calibrated. Several trial runs were made on parts of the site to test the machine's effectiveness in the site's soils. Equipment settings and other pertinent logistical attributes included the following:

- Time Window: 50.7 ns
- Number of Stacks: 4
- Number of Samples: 412
- Sampling Frequency: 7,462.13 MHz
- Antenna: 500 MHz shielded
- Antenna Separation: 0.18 m
- Trigger: 0.04 m
- Radargram orientation: Block A-South to North; Block B-West to East; Block C-West to East
- Radargram progress: Block A-West to East; Block B-South to North; Block C-North to South
- Radargram Spacing: 50 cm
- Total Radargrams: Block A- 42; Block B-28

Weather conditions at the time of the survey were drought. No precipitation had fallen in the area for at least two weeks, so residual rainfall as shallow groundwater was not a significant issue. Furthermore, most of the area of Blocks A and B was covered in high grass. Soils in both GPR blocks are comprised of sandy loam and sand grading to sandy clay. The lowest portion of GPR Block A may contain a mantle of alluvial sediment.

GPR Block A was located in the pasture at 9OC43. This GPR block examined an area 25 m East-West by 21 m North-South. Radargrams were collected from west to east and progressed from north to south, as diagramed in Figure 2. The starting point for Block A (Northwestern corner) was at UTM Zone 17 S 287232E, 3746080N (WGS84).

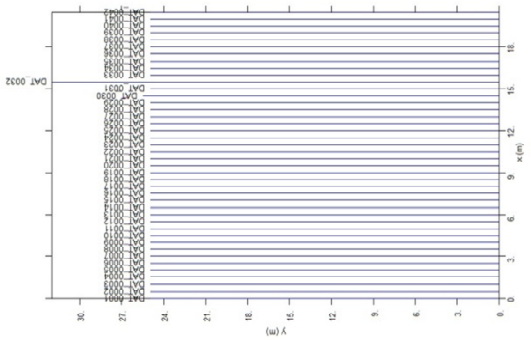

Figure 2. Schematic of Radargrams in GPR Block A, 9OC43 (Northwestern corner is 0,0).

GPR Block B was located at the margin of the pasture and wooded parts of 9OC43. This GPR block was irregular in shape and examined an area 16 m East-West by 14 m North-South. Radargrams were collected from east to west and progressed from south to north, as diagramed in Figure 3. The starting point for Block B (Southwest corner) was at UTM Zone 17 S 287232 E, 3746059N.

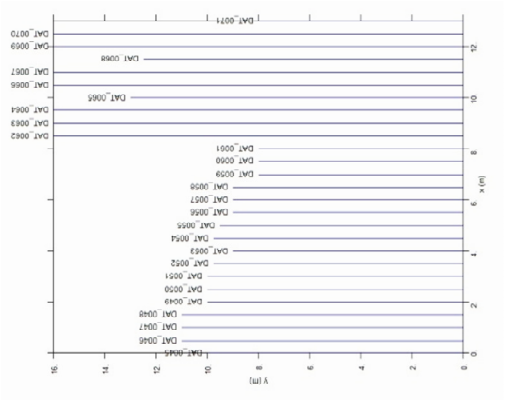

Figure 3. Schematic of Radargrams in GPR Block B, 9OC43 (Southwestern corner is 0.0).

GPR Survey Results

GPR BLOCK A---Figure 4 shows a plan view of GPR reflections in Block A at approximately 30 cm depth. This map shows a number of relatively small distinct radar anomalies. These form no apparent architectural pattern. Some of the anomalies may be cultural, while some may represent tree features.

Figure 5 shows a plan view of GPR reflections in Block A at approximately 70 cm depth. This map shows stronger radar reflections in the upper left (southeastern corner) of the grid. This pattern may represent groundwater differences across the sampled area. This map exhibits no apparent architectural pattern or obvious cultural features.

Figure 6 shows an overlay view of GPR reflections in Block A. This view combines data from a range of depths. This map shows differences in radar reflections from the left side (northern edge) of the sample block Radar reflections in the central portion of the sample display a tendency for orientation along a west-east axis, which also agrees with the direction of downward slope. These reflections may represent gullies, agriculturally-related features, or possibly cultural features associated with the historic site.

Figure 7 shows an isometric view of the GPR reflections in Block A.

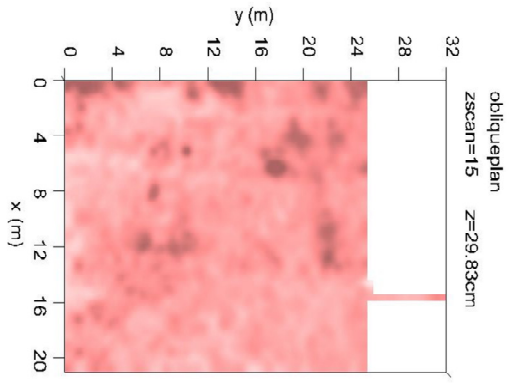

Figure 4. Plan View of GPR Block A,9OC43, ca. 30 cm Depth (Magnetic North is Up).

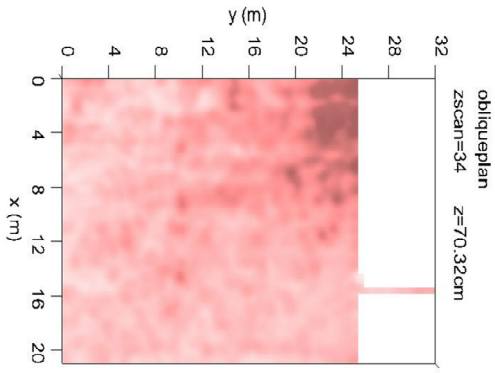

Figure 5. Plan View of GPR Block B, 9OC43, ca. 70 cm Depth.

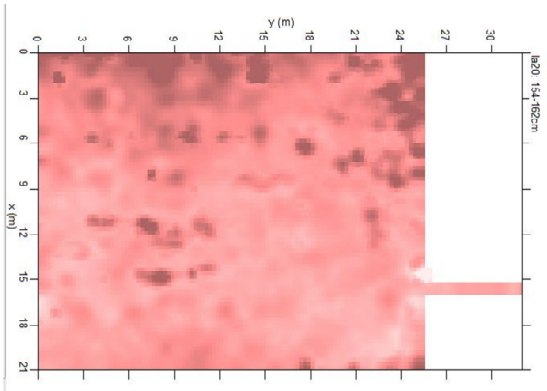

Figure 6. GPR Overlay Plan View of Block A, 9OC43.

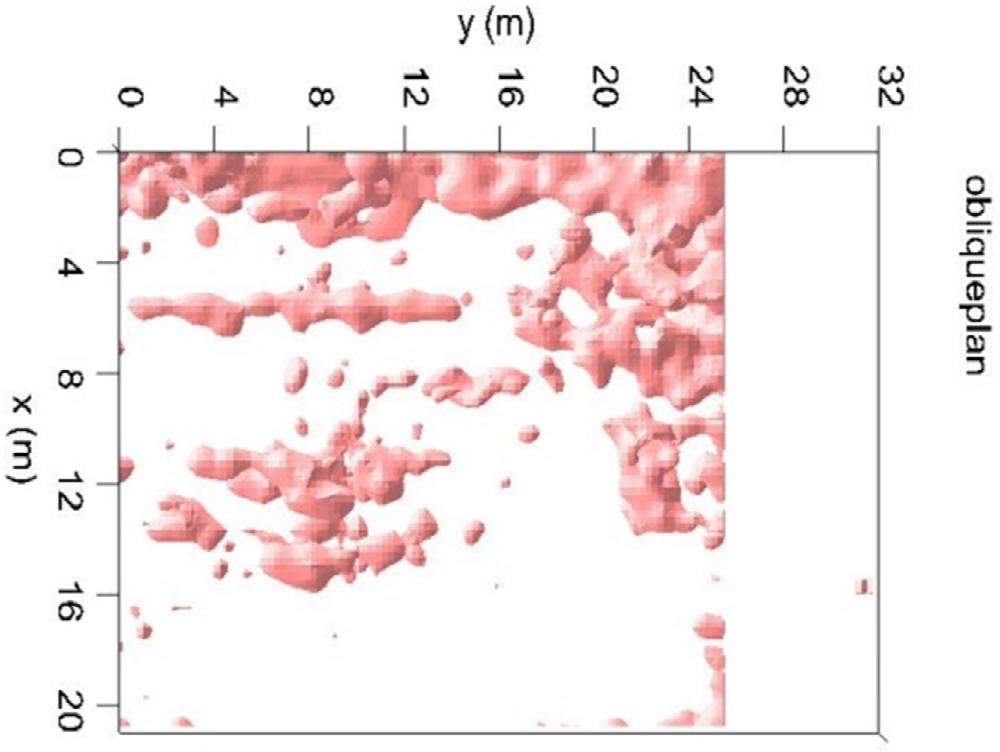

Figure 7. Isometric Plan View of GPR Block A, 9OC43.

GPR BLOCK B---Figure 8 shows a plan view of GPR reflections in Block B at approximately 38 cm depth. Several strong radar anomalies are visible in this view. The lowest one is a long, linear reflection that extends for six meters from about 8 m to the edge of the sample grid. This reflection was created by a downed electric fence that was visible at the surface and partially buried beneath the thick grass. The electricity supply to the fence was inactive at the time of the survey. The standing electric fence served as the northern boundary of the GPR block on its northwestern side.

Figure 9 shows a plan view of GPR reflections in Block B at approximately 87cm depth.
Figure 10 shows an overlay view of GPR reflections in Block B. The overlay image shows a dramatic difference in radar reflections to the west of the electric fence. This area is in hardwoods, whereas the area east of the fence is in pasture.

Figure 11 shows an isometric view of GPR Block B. The downed electric fence is shown by well-defined linear anomaly in this view (marked A at each end).

Figure 12 shows a composite map of GPR Blocks A and B. Figure 13 shows this same map superimposed onto a modern aerial photograph. Figure 14 shows the same map superimposed onto a 1993 aerial photograph (Google Earth 2012).

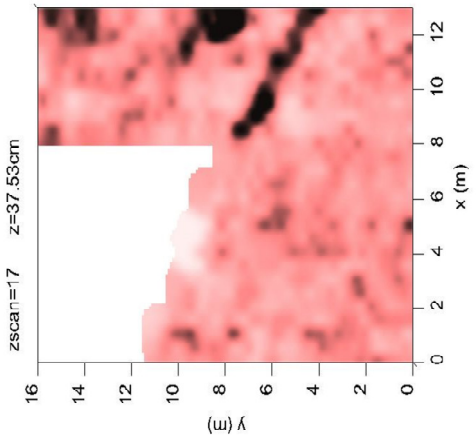

Figure 8. Plan View of GPR Block B, 9OC43, ca. 38 cm Depth (Magnetic North is Up).

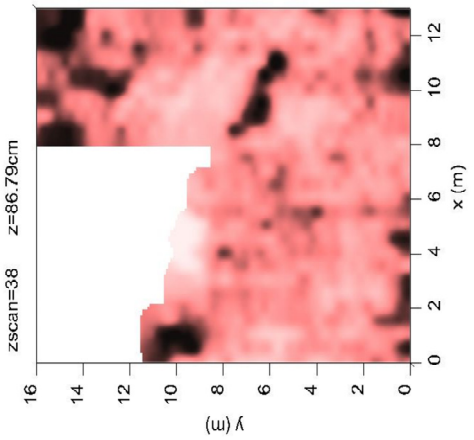

Figure 9. Plan View of GPR Block B, 9OC43, ca. 87 cm Depth.

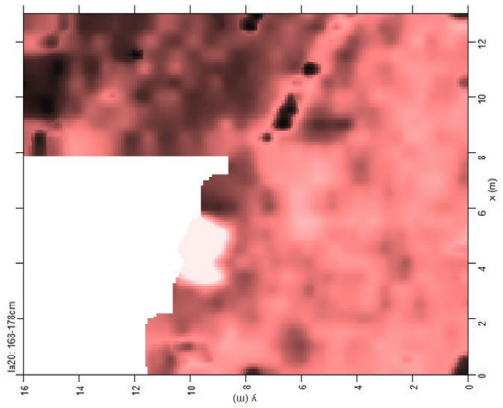

Figure 10. Overlay Plan View of GPR Block B, 9OC43.

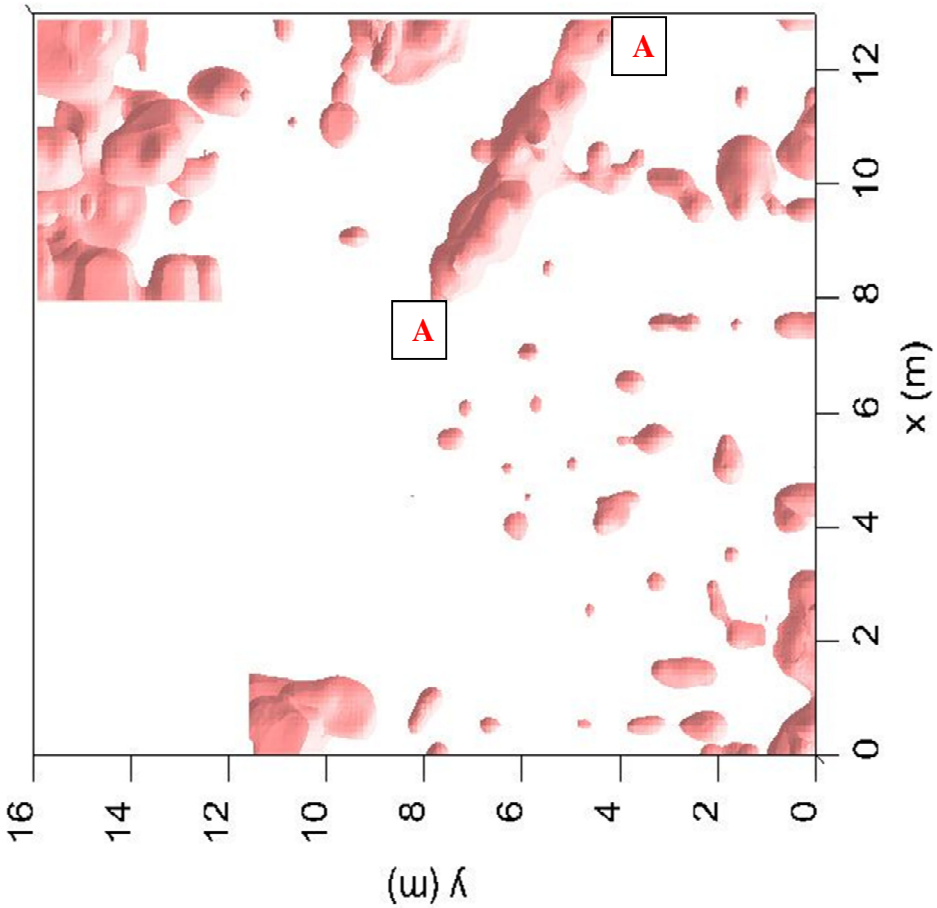

Figure 11. Isometric Plan View of GPR Block B, 9OC43 (A-denotes downed electric fence location).

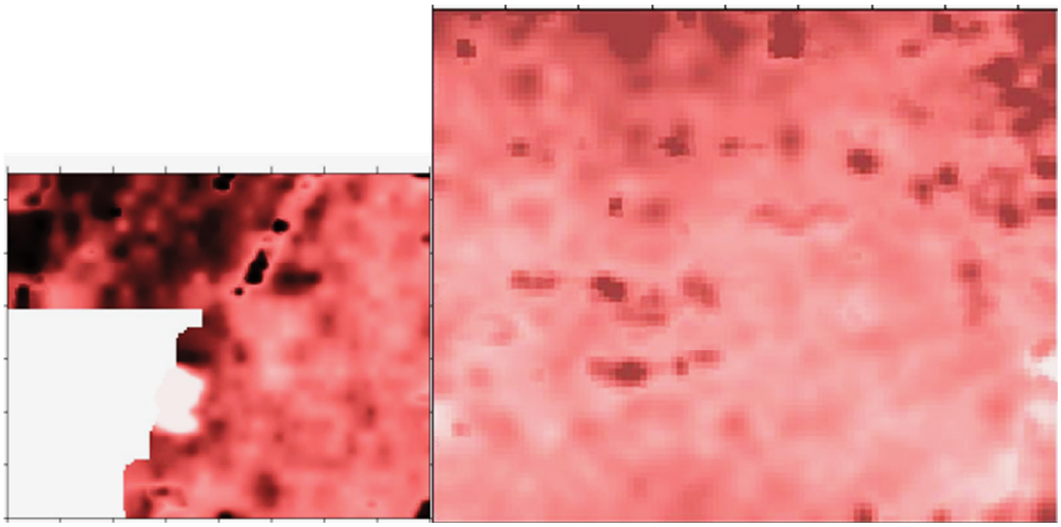

Figure 12. Composite Overlay Plan View of GPR Blocks A and B, 9OC43 (Magnetic North is to Top of Page).

Figure 13. GPR Maps Superimposed on Modern Aerial Photograph of 9OC43 (Google Earth 2012).

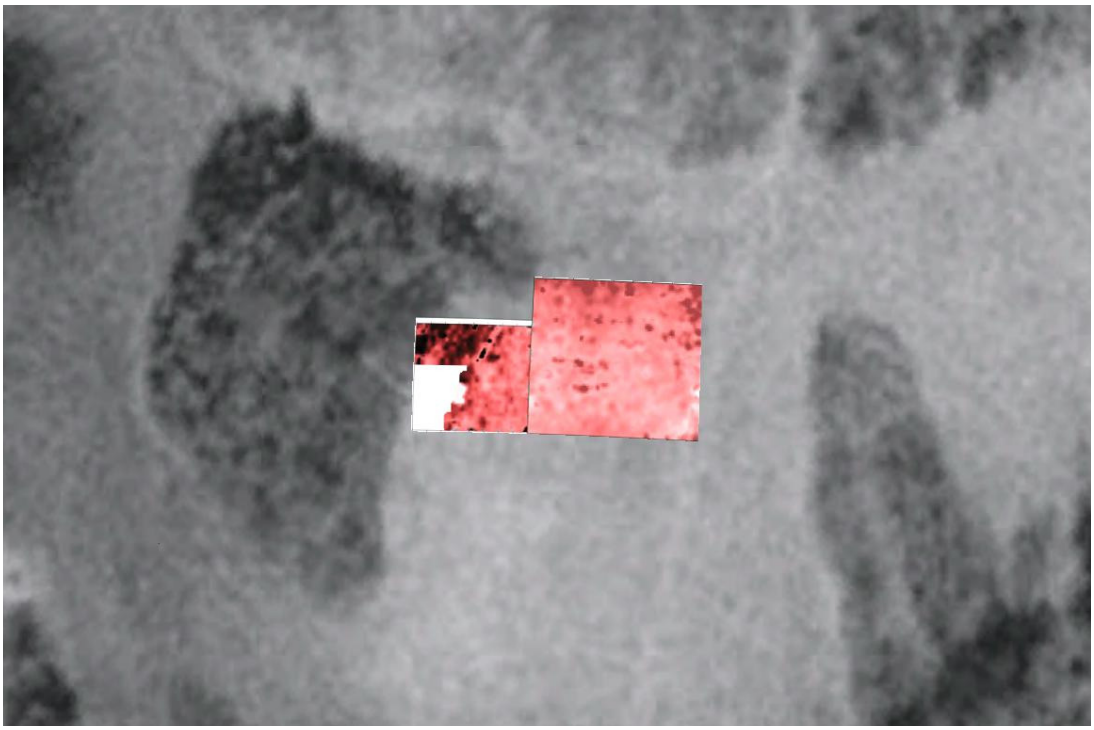

Figure 14. GPR Maps Superimposed on 1993 Aerial Photograph of 9OC43 (Google Earth 2012).

Summary

GPR survey of a portion of Site 9OC43 provides a glimpse of the subsurface characteristics of this potentially significant historic site. A substantial portion of the site was covered by the GPR survey and many radar anomalies were mapped.

References Cited

Conyers, Larry, and Dean Goodman
1997 *Ground-Penetrating Radar. An Introduction for Archaeologists.* Altamira Press, Walnut Creek, California.

Google Earth
2012 Google Earth.

Ledbetter, R. Jerald
1981 9Oc43. Georgia Archaeological Site Form. Georgia Archaeological Site File, Athens, Georgia.

O'Steen, Lisa D.
2012 Search for Fort Mathews, Oconee County, Georgia. DRAFT. Lisa D. O'Steen, Watkinsville, Georgia.